

THEORETICAL MULTIDIMENSIONAL RESOLUTION LIMIT FOR MIMO RADAR BASED ON THE CHERNOFF DISTANCE

N. Duy TRAN^(1,2), Rémy BOYER^(1,2), Alexandre RENAUX⁽¹⁾, Sylvie MARCOS⁽¹⁾ and Pascal LARZABAL⁽²⁾

⁽¹⁾Université Paris-Sud 11 / CNRS / SUPELEC

Laboratoire des Signaux et Systèmes, Supelec, 3, rue Joliot-Curie, 91192 Gif-sur-Yvette, France

⁽²⁾Ecole Normale Supérieure de Cachan

Laboratoire SATIE / CNRS, 61 av. du Président Wilson, 94235 Cachan, France

ABSTRACT

In this paper, we study the behavior of the theoretical multidimensional resolution limit (TMRL) for two closely spaced targets in the context of MIMO Radar with two scenarios: transmitting array and receiving array are widely spaced and collocated. Particularly, we apply the Stein's lemma which links the Chernoff distance and a given probability of error to derive closed-form expression of the TMRL for these models. The theoretical analysis provides interesting characteristics of the TMRL while numerical simulations show that the TMRL is better when amplitudes of two targets are not identical.

Index Terms— MIMO radar, Theoretical Multidimensional Resolution Limit.

1. INTRODUCTION

In recent years, the concept of Multiple-Input Multiple-Output (MIMO) radar has been exploited deeply to improve the performance in target detection and localization [1]. However, not all of its aspects have been fully investigated in the literature. To partially fill this lack, in this paper, we study the behavior of MIMO radar in terms of the Theoretical Resolution Limit (TRL) [2] which is the minimal difference in terms of the parameter of interest to resolve two closely spaced sources. We name theoretical our MRL because the proposed TMRL is independent of a given/considered estimator. The TRL is an important characteristic of a MIMO radar system.

To the best of our knowledge, there are few works concerning the problem of TRL in the context of MIMO radar that have been done. In [3], the TRL (more precisely, the angular resolution limit (ARL)) of a collocated MIMO radar is derived and analyzed using a method based on the resolution of an equation involving the Cramér-Rao bound. In [4], the Multidimensional TRL (TMRL) for two closely spaced targets with a widely spaced MIMO radar is derived by using the Generalized Likelihood Ratio Test (GLRT). Note that, until now, there is none result of the TMRL based on the algorithm criterion or the Cramér-Rao bound in this MIMO radar context due to the difficulty in generalizing the existing mono-dimensional works. In this paper, we propose a different method based on information theory to derive the TMRL of MIMO radar with widely spaced and collocated linear arrays. Particularly, we apply the Stein's lemma [5] [6] which defines the relation between measures (Chernoff distance) of the difference between two probability distributions and the probability of error for a hypothesis test. In the literature,

this lemma has already been used to calculate the relative entropy to study detection performance and to design waveform for MIMO radar in [7] [8] and for multi-static radar in [9]. Besides, in [10], the ARL on resolving two closely spaced polarized sources using vector-sensor arrays is also studied by using the relative entropy.

2. PROBLEM SETUP

2.1. Widely spaced MIMO radar setup

We consider here a MIMO radar system with widely spaced linear arrays ¹ in the case of two point targets. The numbers of antennas in transmitter and receiver are denoted N_T and N_R , respectively. The distances between the i -th sensor w.r.t. a reference are denoted by $d_i^{(T)}$ and $d_i^{(R)}$ for the transmitter and the receiver, respectively. Each point target is located by two parameters: the angle-of-departure denoted by θ_m^T and the angle-of-arrival denoted by θ_m^R , $m = 1, 2$. In this context, the signal at the receiver of such a MIMO radar for the l -th pulse is given by

$$\mathbf{X}_l = \sum_{m=1}^2 \rho_m \exp(j2\pi f_m l) \mathbf{a}_R(\omega_m^{(R)}) (\mathbf{a}_T(\omega_m^{(T)}))^T \mathbf{S} + \mathbf{W}_l \quad (1)$$

where $l = 0 \dots L - 1$ with L is the number of transmitted pulses, and ρ_m , f_m denote the complex amplitude related to the radar-cross-section (RCS) of the target and the normalized Doppler frequency of the m -target, respectively. The steering vectors have the following structures $\mathbf{a}_T(\omega_m^{(T)}) = [\exp(j\omega_m^{(T)} d_1^{(T)}) \dots \exp(j\omega_m^{(T)} d_{N_T}^{(T)})]^T$, and $\mathbf{a}_R(\omega_m^{(R)}) = [\exp(j\omega_m^{(R)} d_1^{(R)}) \dots \exp(j\omega_m^{(R)} d_{N_R}^{(R)})]^T$ where $\omega_m^{(T)} = \frac{2\pi}{\lambda} \sin \theta_m^T$, and $\omega_m^{(R)} = \frac{2\pi}{\lambda} \sin \theta_m^R$ with λ denoting the wavelength. The matrix $\mathbf{S} = [\mathbf{s}_1 \dots \mathbf{s}_{N_T}]^T$ contains N_T transmitted waveforms where each waveform is a vector of T snapshots. We assume that these waveforms are orthogonal so that $\frac{1}{T} \mathbf{S} \mathbf{S}^H = \mathbf{I}_{N_T}$ [1]. The noise matrix for the l -th pulse \mathbf{W}_l is assumed to be independent and identically distributed symmetric complex Gaussian with zero-mean and covariance matrix $\sigma^2 \mathbf{I}_{N_R}$. The output of (1) after matched filtering is given by $\mathbf{y}_l = \text{vec}(\mathbf{Y}_l) = \frac{1}{\sqrt{T}} \text{vec}(\mathbf{X}_l \mathbf{S}^H)$. The observation can then be rewritten as a PARAFAC model [3, 11]:

$$\mathbf{y} = [\mathbf{y}_0^T \dots \mathbf{y}_{L-1}^T]^T = \sum_{m=1}^2 \alpha_m \mathbf{c}(f_m) \otimes \mathbf{a}_T(\omega_m^{(T)}) \otimes \mathbf{a}_R(\omega_m^{(R)}) + \mathbf{z}, \quad (2)$$

where $\alpha_m = \sqrt{T} \rho_m$, $\mathbf{z} = [\mathbf{z}_0^T \dots \mathbf{z}_{L-1}^T]^T$ with $\mathbf{z}_l = \text{vec}(\frac{1}{\sqrt{T}} \mathbf{W}_l \mathbf{S}^H)$ and $\mathbf{c}(f_m) = [1 \exp(i2\pi f_m) \dots \exp(i2\pi f_m(L-1))]^T$ in which

¹the collocated MIMO radar scenario is tackled in Appendix 6.2.

This project was funded by both région Île-de-France and DIGITEO Research Park and by NEWCOM++.

\otimes denotes the Kronecker product. Since \mathbf{W}_l is assumed to be i.i.d. symmetric complex Gaussian with zero-mean and covariance matrix $\sigma^2 \mathbf{I}_{N_R}$, we obtain that $E\{\mathbf{z}\mathbf{z}^H\} = \sigma^2 \mathbf{I}_{LN_T N_R}$. Consequently, the likelihood of the observations \mathbf{y} is complex Gaussian distributed with mean $\sum_{m=1}^2 \alpha_m \mathbf{c}(f_m) \otimes \mathbf{a}_T(\omega_m^{(T)}) \otimes \mathbf{a}_R(\omega_m^{(R)})$ and covariance $\sigma^2 \mathbf{I}_{LN_T N_R}$.

2.2. TMRL based on a detection hypothesis test

If we denote $\delta_T = \omega_2^{(T)} - \omega_1^{(T)}$ and $\delta_R = \omega_2^{(R)} - \omega_1^{(R)}$, the problem of resolving two closely spaced sources can be formulated as a binary hypothesis test as follows:

$$\begin{cases} \mathcal{H}_0 : (\delta_T, \delta_R) = (0, 0), \\ \mathcal{H}_1 : (\delta_T, \delta_R) \neq (0, 0). \end{cases} \quad (3)$$

Assume that δ_T and δ_R are small, by using the first-order Taylor expansion around the so-called center parameters $\omega_c^{(T)} = \frac{\omega_1^{(T)} + \omega_2^{(T)}}{2}$ and $\omega_c^{(R)} = \frac{\omega_1^{(R)} + \omega_2^{(R)}}{2}$, hence, $\omega_1^{(T)} = \omega_c^{(T)} - \frac{\delta_T}{2}$, $\omega_2^{(T)} = \omega_c^{(T)} + \frac{\delta_T}{2}$, $\omega_1^{(R)} = \omega_c^{(R)} - \frac{\delta_R}{2}$, and $\omega_2^{(R)} = \omega_c^{(R)} + \frac{\delta_R}{2}$, one can obtain the linear approximation of (2) as follows

$$\mathbf{y} \simeq \mathbf{G}\mathbf{Q}\boldsymbol{\delta} + \mathbf{z} \quad (4)$$

where $\boldsymbol{\delta} = [1 \ \delta_R \ \delta_T \ \delta_R]^T$, where $\mathbf{Q} = \text{Diag}(\alpha_1 + \alpha_2, \frac{j}{2}(\alpha_2 - \alpha_1), \frac{j}{2}(\alpha_2 - \alpha_1), -\frac{1}{4}(\alpha_1 + \alpha_2))$, and where $\mathbf{G} = [\mathbf{g}_1 \ \mathbf{g}_2 \ \mathbf{g}_3 \ \mathbf{g}_4]$ with $\mathbf{g}_1 = \mathbf{c}(f) \otimes \mathbf{a}_T(\omega_c^{(T)}) \otimes \mathbf{a}_R(\omega_c^{(R)})$, $\mathbf{g}_2 = \mathbf{c}(f) \otimes \dot{\mathbf{a}}_T(\omega_c^{(T)}) \otimes \mathbf{a}_R(\omega_c^{(R)})$, $\mathbf{g}_3 = \mathbf{c}(f) \otimes \mathbf{a}_T(\omega_c^{(T)}) \otimes \dot{\mathbf{a}}_R(\omega_c^{(R)})$, $\mathbf{g}_4 = \mathbf{c}(f) \otimes \dot{\mathbf{a}}_T(\omega_c^{(T)}) \otimes \dot{\mathbf{a}}_R(\omega_c^{(R)})$. Let $\boldsymbol{\delta}_0 = [1 \ 0 \ 0 \ 0]^T$, then (3) can be rewritten as:

$$\begin{cases} \mathcal{H}_0 : \mathbf{y} \sim \mathcal{CN}(\mathbf{G}\mathbf{Q}\boldsymbol{\delta}_0, \sigma^2 \mathbf{I}), \\ \mathcal{H}_1 : \mathbf{y} \sim \mathcal{CN}(\mathbf{G}\mathbf{Q}\boldsymbol{\delta}, \sigma^2 \mathbf{I}). \end{cases} \quad (5)$$

3. STEIN'S LEMMA BASED ANALYSIS OF TMRL

3.1. Chernoff distance for detection test (5)

From the Stein's lemma [5] [6], we have the asymptotic² relation between the Chernoff distance (CD) relying the two probability density functions (pdf) and a given probability of error for a hypothesis test as follows $\mathcal{CD}(p(\mathbf{y}|\mathcal{H}_0)||p(\mathbf{y}|\mathcal{H}_1)) = -\ln(P_e)$ where the Chernoff distance is defined as $\mathcal{CD}(p(\mathbf{y}|\mathcal{H}_0)||p(\mathbf{y}|\mathcal{H}_1))$, and where P_e denotes a given probability of error. In our context, the Chernoff distance can be calculated as a function of δ_T and δ_R as follows (see the Appendix 6.1)

$$\begin{aligned} \mathcal{CD} &= \frac{L}{16\sigma^2} \left(N_R |\alpha_2 - \alpha_1|^2 \sum_{n_t=1}^{N_T} (d_{n_t}^{(T)})^2 \delta_T^2 + 2 |\alpha_2 - \alpha_1|^2 \right. \\ &\quad \left. \sum_{n_t=1}^{N_T} d_{n_t}^{(T)} \sum_{n_r=1}^{N_R} d_{n_r}^{(R)} \delta_T \delta_R + N_T |\alpha_2 - \alpha_1|^2 \sum_{n_r=1}^{N_R} (d_{n_r}^{(R)})^2 \delta_R^2 \right. \\ &\quad \left. + \frac{1}{4} |\alpha_2 + \alpha_1|^2 \sum_{n_t=1}^{N_T} (d_{n_t}^{(T)})^2 \sum_{n_r=1}^{N_R} (d_{n_r}^{(R)})^2 \delta_T^2 \delta_R^2 \right). \end{aligned} \quad (6)$$

²Note that this assumption is not severe in the context of MIMO radar since we generally dispose of a large ($LN_T N_R$) number of observations.

The behavior of the \mathcal{CD} seems hard to study for general array geometries so our analysis will be focused on symmetric (possibly non-uniform) arrays.

3.2. Symmetric array analysis

We here consider the case where both arrays are assumed to be central-symmetric linear and the center of both arrays is chosen as the reference point, i.e. $\sum_{n_t=1}^{N_T} d_{n_t}^{(T)} = 0$ and $\sum_{n_r=1}^{N_R} d_{n_r}^{(R)} = 0$. Denoting $\sigma_T^2 = \frac{1}{N_T} \sum_{n_t=1}^{N_T} (d_{n_t}^{(T)})^2$ and $\sigma_R^2 = \frac{1}{N_R} \sum_{n_r=1}^{N_R} (d_{n_r}^{(R)})^2$, the expression of the CD can be rewritten as

$$\begin{aligned} \mathcal{CD} &= \frac{LN_T N_R}{16\sigma^2} \left(|\alpha_2 - \alpha_1|^2 \sigma_T^2 \delta_T^2 + |\alpha_2 - \alpha_1|^2 \sigma_R^2 \delta_R^2 \right. \\ &\quad \left. + \frac{1}{4} |\alpha_2 + \alpha_1|^2 \sigma_T^2 \sigma_R^2 \delta_T^2 \delta_R^2 \right). \end{aligned} \quad (7)$$

3.3. Analysis w.r.t the amplitudes

We consider two cases with regard to the relation between amplitude coefficients α_1 and α_2 . We also denote the signal to noise ratio in dB by $SNR = 10 \log_{10} \left(\frac{|\alpha_1|^2 + |\alpha_2|^2}{2\sigma^2} \right)$.

1. If $\alpha_1 = \alpha_2 = \alpha$, equation (7) becomes

$$\frac{LN_T N_R}{32\sigma^2} |\alpha|^2 \sigma_T^2 \sigma_R^2 \delta_T^2 \delta_R^2 = -\ln(P_e). \quad (8)$$

Consider δ_T as fixed and $\delta_T > 0$, $\delta_R > 0$, one obtains δ_R in function of δ_T as follows

$$\delta_R = \frac{4\sqrt{-2\ln(P_e)} 10^{-\frac{SNR}{20}}}{\delta_T \sigma_T \sigma_R \sqrt{LN_T N_R}}. \quad (9)$$

The locus of TMRL in this case is a rectangular parabola. In this scenario, we have $\delta_R = O(1/\delta_T)$ and $\delta_T = O(1/\delta_R)$ which mean that if we have a small resolution along the transmission (resp. reception) array, we have a large resolution along the reception (resp. transmission) array. It is easy to see that δ_R is minimized when both $N_T \sigma_T^2$ and $N_R \sigma_R^2$ are maximized. For antennas with fixed apertures, the maxima happens when the elements of both arrays are placed as far as possible w.r.t the reference points (i.e. the centers of the arrays in the considered geometry).

2. If $\alpha_1 \neq \alpha_2$, since the resolution limits are considered to be small, i.e. $\delta_T \ll 1$ and $\delta_R \ll 1$, the term containing $\delta_T^2 \delta_R^2$ in (7) can be omitted and the Stein's lemma can be rewritten as

$$\frac{\delta_T^2}{d_T^2} + \frac{\delta_R^2}{d_R^2} = 1, \quad (10)$$

where $d_T^2 = \frac{-16\sigma^2 \ln(P_e)}{LN_T N_R |\alpha_2 - \alpha_1|^2 \sigma_T^2}$ and $d_R^2 = \frac{-16\sigma^2 \ln(P_e)}{LN_T N_R |\alpha_2 - \alpha_1|^2 \sigma_R^2}$. Equation (10) means that the locus of δ_T and δ_R is an ellipse centered at $(0, 0)$ whose the axes are $2d_T$ and $2d_R$. Without loss of generality, if we consider δ_T fixed and assume that $\delta_R > 0$, one obtains δ_R in function of δ_T as follows

$$\delta_R = d_R \sqrt{1 - \frac{\delta_T^2}{d_T^2}}, \quad (11)$$

under the condition $\delta_T^2 < d_T^2$. Note that if $\sigma_T^2 = \sigma_R^2$, i.e. $d_T^2 = d_R^2 = d^2$, (10) becomes $\delta_T^2 + \delta_R^2 = d^2$ which means that the locus in this case is a circle.

4. NUMERICAL RESULTS

In this Section, some simulations are presented to analyse the behavior of the TMRL. The scenario is the following: the transmit and the receive arrays are uniform linear arrays of $N_T = 4$ and $N_R = 10$ sensors, respectively, with inter-element spacing (in unit of wavelengths) is 0.5, the probability of error is fixed: $P_e = 0.02$, and the number of pulses $L = 10$. First, figure 1 plots the locus of δ_T and δ_R in both case $\alpha_1 = \alpha_2$ and $\alpha_1 \neq \alpha_2$. The locus of δ_T and δ_R is the curve obtained by intersecting the surface $z = CD(\delta_T, \delta_R)$ with the plane $z = -\ln(P_e)$. One can see that the locus in the case $\alpha_1 = \alpha_2$ is a rectangular hyperbola while the locus in the case $\alpha_1 \neq \alpha_2$ is an ellipse. Next, figure 2 plots δ_R versus δ_T when $SNR = 40$

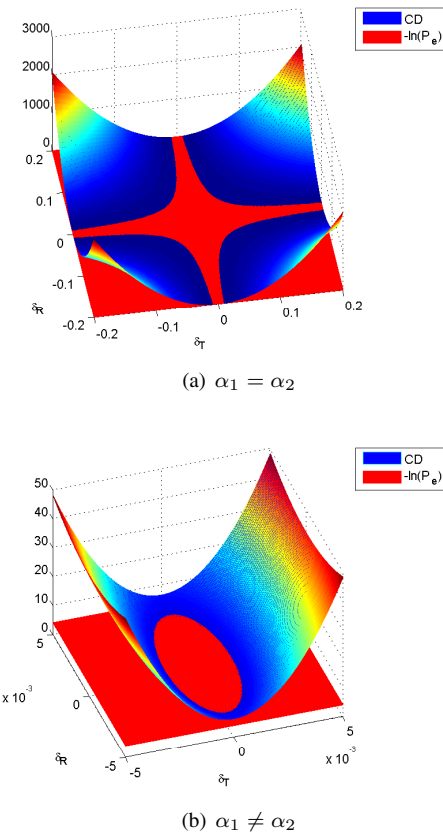


Fig. 1. CD with respect to δ_T and δ_R for $SNR = 40, $P_e = 0.02$.$

in both cases $\alpha_1 = \alpha_2$ and $\alpha_1 \neq \alpha_2$. Note that, in figure 2(a), we also draw a vertical line that divides the curve into two regions where $\delta_R > \delta_T$ on the left hand and $\delta_R < \delta_T$ on the right hand. The value of the TMRL at the intersection between the vertical line and the curve can be analytically derived and is given by

$$\delta_T = \delta_R = \frac{d_T d_R}{\sqrt{d_T^2 + d_R^2}} = \sqrt{\frac{-16\sigma^2 \ln(P_e)}{LN_T N_R |\alpha_2 - \alpha_1|^2 (\sigma_T^2 + \sigma_R^2)}}.$$

We can see here a trade-off between δ_T and δ_R . Comparing fig. 2(a) to fig. 2(b), we can see that when $\alpha_1 \neq \alpha_2$, one obtains better resolution limits than in the case $\alpha_1 = \alpha_2$. Finally, we present a comparison between the collocated arrays context (TRL) and the widely spaced arrays context (TMRL). Particularly, we plot in figure

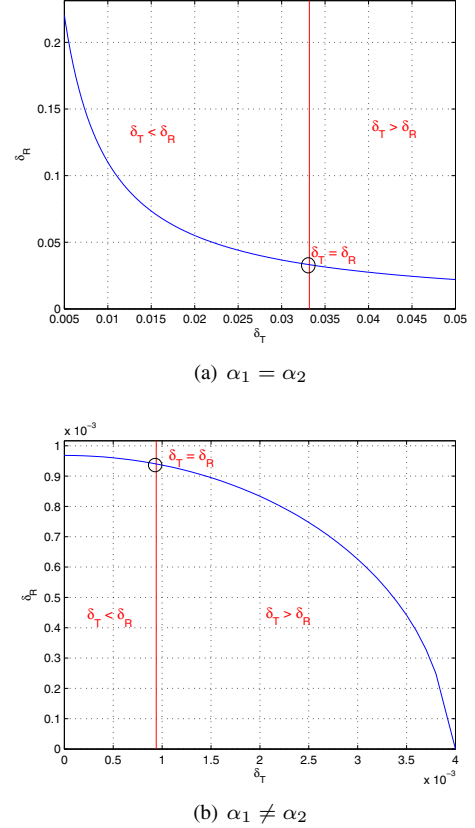


Fig. 2. δ_R versus δ_T for $SNR = 40, $P_e = 0.02$$

3, δ_R versus SNR (δ_T is considered fixed) for the case of the TMRL and δ versus SNR for the case of the TRL with two configurations: (A) $N_T = 4$ and $N_R = 10$ and (B) $N_T = 10$ and $N_R = 4$ and in two scenarios: $\alpha_1 = \alpha_2$ and $\alpha_1 \neq \alpha_2$. By resolving the equation $\delta_R = \delta$ for a given δ_T , we obtain that $\delta_R > \delta$ when $SNR \in [0, SNR_t]$ and $\delta_R < \delta$ when $SNR \in [SNR_t, \infty]$ where SNR_t is given by:

$$\begin{cases} \alpha_1 = \alpha_2 = \alpha : SNR_t = 10 \log_{10} \left(\frac{-16 \ln(P_e)}{\delta_T^2 \sigma_T^2 \sigma_R^2 L N_T N_R} \right), \\ \alpha_1 \neq \alpha_2 : SNR_t = 10 \log_{10} \left(\frac{-16 \ln(P_e) (|\alpha_1|^2 + |\alpha_2|^2)}{\delta_T^2 (\sigma_T^2 + \sigma_R^2) |\alpha_2 - \alpha_1|^2 L N_T N_R} \right). \end{cases}$$

5. CONCLUSIONS

In this paper, we have derived a closed-form expression of the Chernoff distance for a MIMO Radar with widely spaced linear arrays, then, we have applied the Stein's lemma to obtain the TMRL for two closely spaced targets. The analysis has provided interesting characteristics of the TMRL in this context. It has been seen that the behavior of TMRL is different in two cases $\alpha_1 = \alpha_2$ and $\alpha_1 \neq \alpha_2$. Numerical results have shown that the TMRL is better when amplitudes of two targets are not identical.

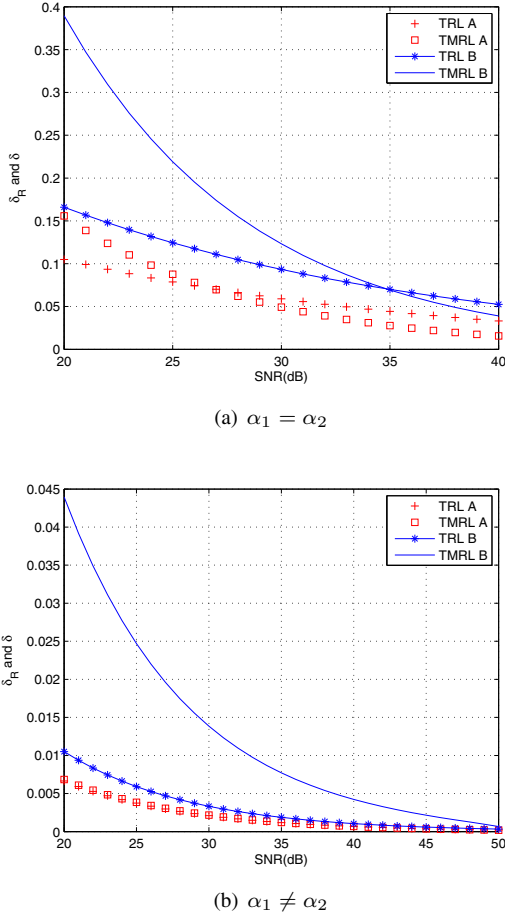


Fig. 3. δ_R and δ versus SNR for $P_e = 0.02$

6. APPENDIX

6.1. Derivation of \mathcal{CD}

The CD between two Gaussian distributions with parameterized means, $\mathbf{y}|\mathcal{H}_0 \sim \mathcal{CN}(\boldsymbol{\mu}_0, \sigma^2 \mathbf{I})$ and $\mathbf{y}|\mathcal{H}_1 \sim \mathcal{CN}(\boldsymbol{\mu}_1, \sigma^2 \mathbf{I})$, is given by [5]

$$\mathcal{CD}(p(\mathbf{y}|\mathcal{H}_0)||p(\mathbf{y}|\mathcal{H}_1)) = \max_{0 \leq k \leq 1} -\log \eta(k), \quad (12)$$

where

$$\begin{aligned} \eta(k) &= \int_{\Omega} [p(\mathbf{y}|\mathcal{H}_0)]^{1-k} [p(\mathbf{y}|\mathcal{H}_1)]^k d\mathbf{y} \\ &= \int_{\Omega} \frac{1}{\pi^{LN_T N_R} |\sigma^2 \mathbf{I}|} \exp \left(-\frac{1-k}{\sigma^2} (\mathbf{y} - \boldsymbol{\mu}_0)^H (\mathbf{y} - \boldsymbol{\mu}_0) \right. \\ &\quad \left. - \frac{k}{\sigma^2} (\mathbf{y} - \boldsymbol{\mu}_1)^H (\mathbf{y} - \boldsymbol{\mu}_1) \right) d\mathbf{y}. \end{aligned} \quad (13)$$

$$= \exp \left(\frac{(k-1)k}{\sigma^2} \|\boldsymbol{\mu}_1 - \boldsymbol{\mu}_0\|^2 \right). \quad (14)$$

Consequently, (12) can be rewritten as

$$\mathcal{CD}(p(\mathbf{y}|\mathcal{H}_0)||p(\mathbf{y}|\mathcal{H}_1)) = \max_{0 \leq k \leq 1} -\frac{(k-1)k}{\sigma^2} \|\boldsymbol{\mu}_1 - \boldsymbol{\mu}_0\|^2. \quad (15)$$

Since $\frac{1}{\sigma^2} (\boldsymbol{\mu}_1 - \boldsymbol{\mu}_0)^H (\boldsymbol{\mu}_1 - \boldsymbol{\mu}_0)$ does not depend on k and it is easy to see that $-(k-1)k$ is maximized when $k = 1/2$, the Chernoff's distance between two Gaussian distributions with parameterized means is given by $\mathcal{CD}(p(\mathbf{y}|\mathcal{H}_0)||p(\mathbf{y}|\mathcal{H}_1)) = \frac{1}{4\sigma^2} \|\boldsymbol{\mu}_1 - \boldsymbol{\mu}_0\|^2$. In our context, we have $\boldsymbol{\mu}_0 = \mathbf{GQ}\boldsymbol{\delta}_0$ and $\boldsymbol{\mu}_1 = \mathbf{GQ}\boldsymbol{\delta}$, consequently, one obtains (6).

6.2. Collocated MIMO radar

In the context of collocated MIMO radar, each point target is now located by only one angle ω_m , $m = 1, 2$, hence, the problem of TMRL becomes mono-dimensional, i.e., $\delta_T = \delta_R = \delta$. After some calculations, the analysis w.r.t the amplitudes for this context is simplified as follows:

1. $\alpha_1 = \alpha_2 = \alpha$: $\delta = \sqrt{\frac{-32 \ln(P_e) 10^{-\frac{SNR}{10}}}{LN_T N_R \sigma_T^2 \sigma_R^2}}$
2. $\alpha_1 \neq \alpha_2$: $\delta = \sqrt{\frac{-16 \sigma^2 \ln(P_e)}{LN_T N_R |\alpha_2 - \alpha_1|^2 (\sigma_T^2 + \sigma_R^2)}}$

7. REFERENCES

- [1] J. Li and P. Stoica, *MIMO Radar Signal Processing*. New York: Wiley, 2009.
- [2] A. J. den Dekker and A. van den Bos, "Resolution, a survey," *J. Opt. Soc. Amer.*, vol. 14, pp. 547–557, 1997.
- [3] R. Boyer, "Performance bounds and angular resolution limit for the moving collocated MIMO radar," *IEEE Transactions on Signal Processing*, vol. 59, no. 4, pp. 1539–1552, Apr. 2011.
- [4] M. N. El Korso, R. Boyer, A. Renaux, and S. Marcos, "Statistical resolution limit for source localization in a MIMO context," in *Proc. of IEEE International Conference on Acoustics, Speech, and Signal Processing (ICASSP)*, Prague, Czech Republic, May 2011.
- [5] T. Cover and J. Thomas, *Elements of Information Theory*. New York: Wiley.
- [6] H. Chernoff, "Large-sample theory: parametric case," *Ann. Math. Statist.*, vol. 28, pp. 1–22, 1956.
- [7] J. Tang, N. Li, Y. Wu, and Y. Peng, "On detection performance of MIMO radar: A relative entropy-based study," *IEEE Signal Processing Letters*, vol. 16, no. 3, pp. 184–187, Mar. 2009.
- [8] B. Tang, J. Tang, and Y. Peng, "MIMO radar waveform design in colored noise based on information theory," *IEEE Transactions on Signal Processing*, vol. 58, no. 9, pp. 4684–4697, Sep. 2010.
- [9] S. Kay, "Waveform design for multistatic radar detection," *IEEE Transactions on Aerospace and Electronic Systems*, vol. 45, no. 3, pp. 1153–1166, Jul. 2009.
- [10] D. T. Vu, M. N. El Korso, R. Boyer, A. Renaux, and S. Marcos, "Angular resolution limit for vector-sensor arrays: Detection and information theory approaches," in *Proc. of IEEE Workshop on Statistical Signal Processing SSP*, Nice, France, Jul. 2011.
- [11] D. Nion and N. D. Sidiropoulos, "Tensor algebra and multidimensional harmonic retrieval in signal processing for MIMO radar," *IEEE Transactions on Signal Processing*, vol. 58, no. 11, pp. 5693–5705, Nov. 2010.